MATHEMATICAL MODELING AND COMPUTING, Vol. 9, No. 2, pp. 416–430 (2022)

Mathematical modeling of non-stationary gas flow modes along a linear section of a gas transmission system

Husarova I. H.[1], Tevyashev A. D.[1], Tevyasheva O. A.[2]

[1] *Department of Applied Mathematics, Kharkiv National University of Radio Electronics, 16 Nauky Ave., 61166, Kharkiv, Ukraine*
[2] *Department of Computer Mathematics and Data Analysis, National Technical University "Kharkiv Polytechnic Institute", 2 Kyrpychov Str., 61002, Kharkiv, Ukraine*

(Received 6 November 2020; Revised 22 January 2022; Accepted 24 January 2022)

Article demonstrates the applicability of modeling non-stationary non-isothermal gas flow along a linear section of a gas transmission system by means of using various numerically simulated models and sophisticated numerical techniques. There are described several models of non-stationary non-isothermal regimes of gas flow along the pipeline section. They are included in the considered general model and their comparative analysis is carried out by the virtue of numerical simulation. The finite difference algorithm is used to solve the simultaneous equations of the numerically simulated model for the pipeline section. The results of calculating the gas flow parameters using various models are presented: both with and without taking into account kinetic energy, as well as both with and without taking into account the Joule–Thompson effect. The matter of choosing the appropriate model is discussed. The obtained results can be used at the stage of transfer pipeline system operation in order to develop scientifically well-founded recommendations for improving the safety and efficiency of the pipeline transportation system.

Keywords: *linear section, non-stationary non-isothermal mode of gas flow, modeling, finite difference algorithm.*

2010 MSC: 76N99, 76M20 **DOI:** 10.23939/mmc2022.02.416

1. Introductory note

Having regard to the growth of energy consumption value in the world, it can be said that gas is currently becoming the top chosen energy resource. This growth has been especially observed in the industrial sector, where the share of gas was 20.9% in 2013, is expected to be 22.2% in 2020, and is expected to be 24.6% in 2040 [1].

The increase in world-embracing LNG trade has been the last decade trend. However, the transmission of gas through pipelines, which remains currently the most efficient way of supplying gas, continues to be relevant. Most of the world's reserves currently being produced and developed belong to the so-called conventional gas. Modern technologies for the design, construction, operation and modernization of transfer pipeline systems must be supplemented by numerical techniques for modeling the operational lifetime of the considered pipeline transportation system, including techniques for modeling gas flow regimes in emergency situations or unexpected occurrences, based on the use of numerically simulated models that would consider all the nuances of gas transmission modes. Such supplement to these technologies provides for the firm development of scientifically well-founded recommendations to improve the safety and efficiency of the pipeline transportation system.

This paper presents emergency situations or unexpected occurrences caused by disconnection or connection of large consumers, unsanctioned siphoning or leakage in the pipeline. Such gas flow regimes (GFRs) are non-stationary non-isothermal.

From this perspective, the timeliness of these studies is determined by the need for scientific development and argumentation of both new mathematical models and numerical techniques that would allow carrying out the modeling of gas flow non-stationary processes and using them as a base for management of emergency situations or unexpected occurrences along the linear section (LS) of the gas transmission system (GTS) taking into account boundary conditions (BCs). LS of a GTS is made as pipes connected to a gas pipeline for joining gas-compressor stations. We assume that the LS is a system of pipeline sections (PS) interconnected by shutoff valves (taps) and combined into a single circuit.

2. Literature data analysis and target setting

First and foremost, mathematical models (MMs) of non-stationary non-isothermal gas flow regimes (NNGFRs) along a LS of a GTS were analyzed. For the most part, MMs of NNGFRs along a LS are presented as an interconnected partial differential system [2–8] or integral equations [5] that describe such regimes in a pipeline section. These simultaneous equations are connected either by systems of algebraic equations [2, 4, 7], or partial differential systems [5, 6], or systems of differential and algebraic equations [3], which describe the conditions for matching the parameters of the gas flow at the connections of pipeline sections. The regimes of gas flow through shutoff valves (taps) are set, most commonly, by systems of nonlinear algebraic equations [2, 4, 7, 21]. The primary target in development of MMs of NNGFRs along the LS is selecting a MM for such regimes in a PS. The MM for such regimes can be obtained from the Navier–Stokes basic equations of gas dynamics for the one-dimensional case or from the principal laws of conservation (laws of conservation of mass, momentum and energy). In addition, a MM of NNGFRs in a PS can be presented not only in the form of a partial differential system [2, 22], but also in an integrated form [5]. And at this point, the initial equations of MM [2–22] can be simplified by making certain assumptions, for example, regarding the thermophysical properties of a gas or medium, technical parameters of a pipeline, etc.

An analysis of numerical techniques for solving systems of hyperbolic partial differential equations was carried out. Methods such as the finite difference algorithm with the use of various uniform and non-uniform finite-difference grids [2–8, 12], adaptive methods of implicit finite differences [13], and the method of characteristics (Massau's method, the modified Massau's method) [16], the finite volume method [5, 6, 14], the finite element method, the finite difference method using the Lagrange particle method (is an update of the approach to solving hyperbolic partial differential equations by the method of characteristics) [5, 6], the integro-interpolation method [5, 6], and others, are often used for the obtaining numerical solution of such systems. Each of the specified methods has both advantages and disadvantages.

3. Purpose and objectives of the study

The article object is to choose the mathematical model of NNGFRs along a LS of a gas transmission system, to study the mathematical models of NNGFRs along a LS, which are included in the general MM of NNGFRs along a LS of a GTS, to analyze the results obtained based on numerical modeling and to select the best model in terms of both the accuracy of the description of the processes under consideration and speed-in-action. These models are considered taking into account (without taking into account) various conditions: without taking into account the Joule–Thompson effect and kinetic energy, taking into account the Joule–Thompson effect for the length of the pipeline, taking into account kinetic energy. The finite difference method using a uniform finite-difference grid was chosen as a method for solving a system of differential equations of hyperbolic type with a known non-linear equation (NE) and boundary conditions (BCs) describing the MM of NNGFRs along a LS.

4. Materials and methods for studying the influence of selecting a mathematical model for non-stationary non-isothermal regimes of gas flow along a pipeline section on the processes of modeling such regimes in a linear section of a gas transmission system

4.1. A mathematical model of non-stationary non-isothermal regimes of gas flow along a pipeline section

For the general case of NNGFRs along a LS, which is a cylindrical pipe of constant diameter with rigid walls, it is described by a quasi-linear partial differential system derived from the general Navier–Stokes equations of gas dynamics for the one-dimensional case [4, 7]:

$$\frac{\partial(\rho V)}{\partial t}+\frac{\partial}{\partial x}\left[P+(1+\beta)\rho V^2\right]=-\rho\left[\frac{\lambda|V|V}{2D}+g\frac{dh}{dx}\right], \tag{1}$$

$$\frac{\partial\rho}{\partial t}+\frac{\partial}{\partial x}(\rho V)=0, \tag{2}$$

$$\frac{\partial}{\partial t}(\rho E)+\frac{\partial}{\partial x}\left(\rho V\left(E+\frac{P}{\rho}\right)\right)=\frac{4K}{D}(T_{gr}-T)-\rho V g\frac{dh}{dx}, \tag{3}$$

where $\rho(x,t)$, $V(x,t)$, $T(x,t)$, $P(x,t)$ are specific gravity, velocity, temperature, and pressure of gas; t, x are temporal and spatial coordinate; λ is flow friction characteristic; D is pipe diameter; K is pipe-to-ground heat transmission coefficient; T_{gr} is ground temperature; h is pipe depth; β is Coriolis correction for the uneven velocity distribution in the section; g is gravity acceleration; E is unit mass total energy.

These equations were derived assuming, that there is no mass transfer with the environment, the stationarity of regimes of heat transfer with the environment, thermal properties of the environment were disregarded.

For non-stationary non-isothermal regimes of gas transmission, we can introduce the following assumptions without loss of generality:

— the gas flow velocities are distributed uniformly in cross section, and the Coriolis correction can be disregarded;
— in (1) and (2) equations, we can disregard the change in temperature, since the derivatives of temperature are negligible;
— momentum energy can be disregarded in equation (3), and the Joule–Thompson effect can be disregarded in (3) equation as well.

The (1)–(3) system has to be supplemented with the equation of state:

$$\frac{P}{\rho}=zgRT, \tag{4}$$

where $z(x,t)$ is gas-compressibility factor; R is gas constant.

The (1)–(3) system transforms [4, 7] after application of the relevant manipulations:

$$\frac{\partial W}{\partial t}+\left(1-\alpha TS\frac{W^2}{P^2}\right)\frac{\partial P}{\partial x}+2\alpha TS\frac{W}{T}\frac{\partial W}{\partial x}+\beta TS\frac{W|W|}{P}+\frac{g}{\alpha S}\frac{P}{T}\frac{dh}{dx}=0, \tag{5}$$

$$\frac{\partial P}{\partial t}+\alpha TS\frac{\partial W}{\partial x}=0, \tag{6}$$

$$\frac{\partial T}{\partial t}+\alpha TS\frac{W}{P}\gamma\frac{\partial T}{\partial x}+\alpha S\frac{T^2}{P}(\gamma-1)\frac{\partial W}{\partial x}-\frac{4K}{D}(\gamma-1)\frac{T}{P}(T-T_{gr})-g(\gamma-1)\frac{TW}{P}\frac{dh}{dx}=0, \tag{7}$$

where $\alpha=\frac{zgR}{S}$, $\beta=\frac{\lambda\alpha}{2D}$, $\gamma=\frac{C_p}{C_p-zgR}$, S is sectional area, C_p is gas specific heat, $W(x,t)$ is gas mass flowrate, t is temporal coordinate, x is spatial coordinate.

The (5)–(7) simultaneous equations will be presented in matrix form:

$$\frac{\partial \phi}{\partial t} + B(x,t,\phi)\frac{\partial \phi}{\partial x} = \Phi(x,t,\phi), \tag{8}$$

where

$$B = \begin{bmatrix} 2\alpha TS\dfrac{W}{P} & 1-\alpha TS\dfrac{W^2}{P^2} & 0 \\ \alpha TS & 0 & 0 \\ \alpha S\dfrac{T^2}{P}(\gamma-1) & 0 & \alpha TS\dfrac{W}{P}\gamma \end{bmatrix}, \tag{9}$$

$$\Phi = \begin{bmatrix} -\beta TS\dfrac{W|W|}{P} - \dfrac{g}{\alpha S}\dfrac{P}{T}\dfrac{dh}{dx} \\ 0 \\ -\dfrac{4K}{D}(\gamma-1)\dfrac{T}{P}(T-T_{gr}) - g(\gamma-1)\dfrac{TW}{P}\dfrac{dh}{dx} \end{bmatrix}. \tag{10}$$

In the case when the Joule–Thompson effect is taken into account in the (3) energy equation by gas adiabatic throttling, the (1)–(3) simultaneous equations take the (8) form, where B, Φ matrices have the following form [20]:

$$B = \begin{bmatrix} 2\alpha TS\dfrac{W}{P} & 1-\alpha TS\dfrac{W^2}{P^2} & 0 \\ \alpha TS & 0 & 0 \\ \left(\dfrac{T\gamma}{T-\gamma D_j P}-1\right) & -\dfrac{\alpha S\gamma D_j}{T-\gamma D_j P}\dfrac{T^2W}{P} & \dfrac{\alpha S\gamma}{T-\gamma D_j P}\dfrac{T^2W}{P} \end{bmatrix}, \tag{11}$$

$$\Phi = \begin{bmatrix} -\beta TS\dfrac{W|W|}{P} - \dfrac{g}{\alpha S}\dfrac{P}{T}\dfrac{dh}{dx} \\ 0 \\ -\dfrac{4K(\gamma-1)}{D}\dfrac{T^2(T-T_{gr})}{P(T-PD_j\gamma)} - \dfrac{g(\gamma-1)}{T-PD_j\gamma}\dfrac{T^2W}{P}\dfrac{dh}{dx} \end{bmatrix}, \tag{12}$$

where D_j is Joule–Thomson coefficient (K/Pa). Tables, graphs or empirical formulas are used when determining the Joule–Thompson coefficient for certain values of both temperature and pressure.

In the case when momentum energy is taken into account in the (3) energy equation, the (1)–(3) simultaneous equations take the (8) form, where B, Φ matrices are the next:

$$B = \begin{bmatrix} 2\alpha TS\dfrac{W}{P} & 1-\alpha TS\dfrac{W^2}{P^2} & 0 \\ \alpha TS & 0 & 0 \\ \dfrac{2PT^2}{W}+\dfrac{\alpha ST^2}{P} & -\dfrac{2T}{W} & \dfrac{2\alpha SWT}{P}+\dfrac{2C_P P}{\alpha SW} \end{bmatrix}, \tag{13}$$

$$\Phi = \begin{bmatrix} -\beta TS\dfrac{W|W|}{P} - \dfrac{g}{\alpha S}\dfrac{P}{T}\dfrac{dh}{dx} \\ 0 \\ 2\beta S\dfrac{T^2|W|}{P} - \dfrac{8KP}{D\alpha SW^2}(T-T_{gr}) \end{bmatrix}. \tag{14}$$

In (8), B, Φ are matrices, which elements are given x, t, W, P, T continuous functions of variables differentiable in a certain area of their arguments variation; $\phi(x,t) = (W(x,t), P(x,t), T(x,t))$ is certain continuously-differentiable solution of (8) in $\Lambda = (x,t), x \in [0,L], t \in [0,T_{\max}]$, these matrices are given either by (9)–(10) formulas, or by (11)–(12) formulas, or by (13)–(14) formulas.

Therefore, the NNGFRs are described by a quasilinear system of differential equations of hyperbolic type (8), with the corresponding boundary and initial conditions.

The boundary conditions at the beginning and end of the section are as follows:

$$\begin{cases} \begin{bmatrix} G(0,t) = G^0(t), \\ P(0,t) = P^0(t), \end{bmatrix} \\ T(0,t) = T^0(t), \qquad \text{in case} \quad G(0,t) > 0, \end{cases} \qquad \begin{cases} \begin{bmatrix} G(L,t) = G^1(t), \\ P(L,t) = P^1(t), \end{bmatrix} \\ T(L,t) = T^1(t), \qquad \text{in case} \quad G(L,t) < 0, \end{cases} \tag{15}$$

where $G = WS$ is gas-weight flotation (kg/s), $G^0(t)$, $T^0(t)$, $P^0(t)$, $G^1(t)$, $T^1(t)$, $P^1(t)$ are prescribed functions.

The initial conditions are:

$$W(x,0) = W_0(x), \quad P(x,0) = P_0(x), \quad T(x,0) = T_0(x), \quad x \in (0,L), \tag{16}$$

where $W_0(x)$, $T_0(x)$, $P_0(x)$ are prescribed functions.

Thus wise, it has been possible to obtain mathematical model 1 of NNGFRs along a LS, which is given by (8), (9)–(10), (15)–(16) formulas, mathematical model 2 of NNGFRs along a LS, which is given by (8), (11)–(12), (15)–(16) formulas, mathematical model 3 of NNGFRs along a LS, which is given by (8), (13)–(14), (15)–(16) formulas.

4.2. Mathematical model of gas flow through shut-off valves

It is proposed to choose a model that represents the equations of energy conservation and local pressure loss, describing the modes of natural gas flow through the valve, in the following form [2, 4, 7], as a MM of the regimes for the gas flow through shut-off valves (SVs) (pipeline tap):

$$P_K = P_H - \zeta \frac{Rg}{2F_K^2} \frac{T_K z_K}{P_K} G_H^2, \tag{17}$$

$$T_K = T_H - D_j(P_H - P_K), \tag{18}$$

where T_H, T_K are temperature (K) at the input and output of the valve respectively, P_H, P_K are pressure (Pa) at the input and output of the valve respectively, D_j is Joule–Thomson coefficient (K/Pa), z_K is gas-compressibility factor at the output of the valve respectively, F_K is pipe section area after crossing the valve (m^2), G_H is gas-weight flotation (kg/s) at the input of the valve.

Formula

$$\zeta = \zeta_c \frac{F_K^2}{\varepsilon^2 \left(F_c'\right)^2} + \zeta_K, \tag{19}$$

where ζ_c is coefficient of local hydraulic resistance of compressed flow, ζ_K is coefficient of local hydraulic resistance after crossing the valve, $\varepsilon = \dfrac{F_c}{F_c'}$ is constriction coefficient, F_c is sectional area (m^2) of compressed flow, F_c' is line flow area (m^2) before the flow compression, there is a total resistance coefficient related to the flow in the section F_K.

As a rule, the local resistance coefficient is determined experimentally and is taken from the corresponding tables and graphs in calculations.

4.3. A mathematical model of non-stationary non-isothermal regimes of gas flow along a linear section of a gas transmission system

The LS can be considered as an oriented graph, which edges are PS and SVs, and connections of the PS and SVs are the graph nodes. Consequently, the model of a structure of the LS of GFRs can be defined by means of $G(V, M)$ oriented graph, where V is vertex set of the graph, M is set of edges of the graph. The edges of the graph are places of interconnection of the technological elements. A set of oriented edges $M = M_1 \cup M_2$, where M_1 is a set of oriented graph edges of the relevant PS, M_2 is a set of oriented graph edges of the relevant valves. A vertex set $V = V_1 \cup V_2 \cup V_3 \cup V_4 \cup V_5$, where V_1, V_2, V_3, V_4, V_5 are a set of the PS inputs, a set of intermediate vertex, a set of the PS outputs, a set of inputs and outputs of all valves from M_2 respectively.

The MM of NNGFRs in the LS of a GTS represents interconnected quasilinear systems of partial differential equations corresponding to the i graph edge $G(V,M)$, $\forall i \in M_1$ [4,7]:

$$\frac{\partial \phi^i}{\partial t} + B(x,t,\phi^i)\frac{\partial \phi^i}{\partial x} = \Phi(x,t,\phi^i), \tag{20}$$

where $\phi^i = \big(W^i(x,t), P^i(x,t), T^i(x,t))\big)$, $W^i(x,t)$, $P^i(x,t)$, $T^i(x,t)$ are mass flowrate (kg/m^{2}s), temperature (K), gas pressure (Pa) of i PS.

Equations (20) are supplemented by systems of nonlinear algebraic equations describing the operation modes of a linear crane corresponding to the i graph edge $G(V,M)$, $\forall i \in M_2$ [2,4,7]:

$$P^i(x^{++},t) = P^i(x^+,t) - \zeta^i \frac{Rg}{2(S^j)^2}\frac{T^i(x^{++},t)z^i}{P^i(x^{++},t)}\left(G^i(x^+,t)\right)^2, \tag{21}$$

$$T^i(x^{++},t) = T^i(x^+,t) - D_i\left(P^i(x^+,t) - P^i(x^{++},t)\right), \quad i \in M_2, \quad j \in M_1, \tag{22}$$

where ζ^i is coefficient of local hydraulic resistance, z^i is gas-compressibility factor at the output of the valve, G^i is gas-weight flotation (kg/s) at the valve input, D_i is Joule–Thomson coefficient (K/Pa), S^j is sectional area of the j edge ($j \in M_1$) adjacent to the end of the i edge ($i \in M_2$) corresponding to the valve, x^+, x^{++} are beginning and end of the i edge.

Systems (20), (21)–(22) are interconnected by systems of nonlinear algebraic equations at the intermediate m-vertex ($m \in V_2 \cup V_3 \cup V_4$) of the graph $G(V,M)$:

$$\sum_{j\in V_m^+} G^j(x^{++},t) = \sum_{i\in V_m^-} G^i(x^+,t), \quad m \in V_2, \tag{23}$$

$$P_y^m(t) = P^j(x^{++},t) = P^i(x^+,t), \quad j \in V_m^+, \quad i \in V_m^- \tag{24}$$

$$\sum_{j\in V_m^+}\left(G^j(x^{++},t)\right)^+ T^j(x^{++},t) + \sum_{i\in V_m^-}\left(G^i(x^+,t)\right)^- T^i(x^+,t) = T_c^m\left(\sum_{j\in V_m^+}\left(G^j(x^{++},t)\right)^+ + \sum_{i\in V_m^-}\left(G^i(x^+,t)\right)^-\right) \tag{25}$$

in addition,

$$\begin{aligned} T^j(x^{++},t) &= T_c^m(t), \quad j \in V_m^+ \quad \text{in case} \quad G^j(x^{++},t) < 0, \\ T^i(x^+,t) &= T_c^m(t), \quad j \in V_m^- \quad \text{in case} \quad G^i(x^+,t) > 0, \end{aligned} \tag{26}$$

where x^+ and x^{++} are beginning and end of the i edge, V_m^+ and V_m^- are a set of indices of the edges incoming and outcoming from m graph vertex ($m \in V_2 \cup V_3 \cup V_4$), $G^i(x,t)$, $T^i(x,t)$, $P^i(x,t)$ are mass flowrate, pressure and temperature for the i-edge of the graph, $P_y^m(t)$ is gas pressure in m-vertex, $T_c^m(t)$ is average temperature of the gas flowing out of the m-vertex,

$$(a)^+ = \begin{cases} a, & a > 0 \\ 0, & a \leqslant 0 \end{cases}, \quad (a)^- = \begin{cases} -a, & a < 0 \\ 0, & a \geqslant 0 \end{cases}.$$

These systems correspond to the conditions for matching gas flow parameters at intermediate vertices ($V_2 \cup V_3 \cup V_4$) of the graph $G(V,M)$.

The initial condition is determined by setting the distribution of gas flow parameters (mass flowrate, pressure and temperature) at the initial time moment, i.e.

$$W^i(x,0) = W_0^i(x), \quad P^i(x,0) = P_0^i(x), \quad T^i(x,0) = T_0^i(x), \tag{27}$$

where $x \in \left[x_i^+, x_i^{++}\right]$, $i \in M_1$, $W_0^i(x)$, $P_0^i(x)$, $T_0^i(x)$ are known functions.

Boundary conditions can be specified in various ways [4,7]. As a rule, pressure and temperature are set at the inputs, and gas flow rate is set at the outputs, as time-varying functions.

Now it can be seen that, the mathematical model of NNGFRs in a LS of a GTS is presented by simultaneous equations (20), (21)–(22) and (23)–(26), with non-linear equations of (27) type and various combinations of BCs. In the (20) system, the B, Φ matrices are calculated either by the (9)–(10) formulas, or the (11)–(12) formulas, or the (13)–(14) formulas.

4.4. A numerical technique for solving equations of a mathematical model of non-stationary non-isothermal regimes of gas flow along a pipeline section

Numerical calculation of system (8) with the initial distribution (16) and BSs (15) will be performed by means of a subtended finite-difference scheme having a second order in a spatial variable and a first order in a temporary variable. For this purpose, the $[0, L]$ segment will be divided for n segments of Δx length, and then it is possible to derive $(n+1)$ a point of division $x_i, i = \overline{0, n}$.

In this case, the derivatives in system (8) are replaced by finite-difference formulas:

$$\left.\frac{\partial\phi}{\partial t}\right|_i^k = \frac{\phi_i^k - \phi_i^{k-1}}{\Delta t},\ i = \overline{0,n}, \qquad \left.\frac{\partial\phi}{\partial x}\right|_i^k = \begin{cases} \frac{\phi_1^k - \phi_0^k}{\Delta x},\ i = 0, \\ \frac{\phi_{i+1}^k - \phi_{i-1}^k}{2\Delta x},\ i = \overline{1, n-1}, \\ \frac{\phi_n^k - \phi_{n-1}^k}{\Delta x},\ i = n. \end{cases} \tag{28}$$

The following finite-difference equation system is formed taking into account the (33) and (34) formulas:

$$-\frac{1}{\Delta x}B_0^k\phi_0^k + \frac{1}{\Delta t}\phi_0^k + \frac{1}{\Delta x}B_0^k\phi_1^k = \Phi_0^k + \frac{1}{\Delta t}\phi_0^{k-1},\ i = 0, \tag{29}$$

$$-\frac{1}{2\Delta x}B_i^k\phi_{i-1}^k + \frac{1}{\Delta t}\phi_i^k + \frac{1}{2\Delta x}B_i^k\phi_{i+1}^k = \Phi_i^k + \frac{1}{\Delta t}\phi_i^{k-1},\ i = \overline{1, n-1}, \tag{30}$$

$$-\frac{1}{\Delta x}B_n^k\phi_{n-1}^k + \frac{1}{\Delta t}\phi_n^k + \frac{1}{\Delta x}B_n^k\phi_n^k = \Phi_n^k + \frac{1}{\Delta t}\phi_n^{k-1},\ i = n. \tag{31}$$

The solution of the simultaneous equations (29)–(31) is vector $\phi^k = \left(\phi_0^k, \phi_1^k, \phi_2^k, \ldots, \phi_i^k, \ldots, \phi_n^k\right) = \left(W_0^k, P_0^k, T_0^k, W_1^k, P_1^k, T_1^k, \ldots, W_n^k, P_n^k, T_n^k\right)$.

The system of nonlinear algebraic equations will be solved by the Newton method.

Linear equations system at the s-iteration of the k-time layer is:

$$\left[\frac{\partial\psi^k}{\partial\phi^k}\right]_{\phi^{k,s-1}} \delta\phi^{k,s} = \psi^{k,s-1}, \tag{32}$$

where $\left[\frac{\partial\psi^k}{\partial\phi^k}\right]_{\phi^{k,s-1}}$ is the matrix of Jacobi; $\delta\phi^{k,s}$ is the vector of corrections to the indeterminates at s-iteration; $\psi^{k,s-1}$ is the nullity vector.

The components of the nullity vectors and the components of the matrix of derivatives are found in order to solve these simultaneous equations. The components of the vectors of corrections to the indeterminates at s-iteration of the k-time layer are calculated by means of the linear system.

A numerical technique for solving the equations of the mathematical model of non-stationary non-isothermal regimes of gas flow along the LS of a GTS is described in [4, 7].

5. The results of studies on numerical modeling of NNGFRs in the PS using various mathematical models

We would like to highlight the results of numerical modeling of NNGFRs in the PS using the following examples. The results of calculating the gas flow parameters (flow rate, pressure, temperature) at NNGFRs in the PS obtained using different mathematical models, are compared. These results were obtained using the finite difference algorithm described in 4.4.

The PS having length of $L = 112\,\text{km}$, diameter $D = 1400\,\text{mm}$, section efficiency coefficient $E = 0.95$, wall thickness $\delta = 10\,\text{mm}$, equivalent pipe roughness $K = 0.03\,\text{mm}$, where the thermal capacity is $C_p = 0.655952\,\text{kcal}/(\text{kg K})$, the gas-ground heat transmission coefficient is $k_r = 1.4\,\text{kcal}/(\text{m}^3\,\text{h K})$, the specific gravity of gas is $\Delta = 0.604707$, soil temperature at the depth of the gas pipeline is $t_{gr} = 10^\circ\,\text{C}$, is considered. The subinterval for temporary variable is $\tau = 300\,\text{seconds}$, the number of point of division is $n = 20$, $T_{\max} = 12\,\text{hours}$. The accuracy of calculation is $\varepsilon = 10^{-6}$.

The initial conditions are as follows:

$$P_H = 84.6364456\,\text{atm}, \quad t_H = 40^\circ\text{C}, \quad q = 102.266\,\text{mill.m}^3/\text{day}. \tag{33}$$

A stationary distribution is taken as the initial distribution.

The case of connecting a large consumer from the 200$^{\text{th}}$ minute after the start of the calculation and disconnecting this consumer from the 400$^{\text{th}}$ minute, respectively, is considered. The boundary conditions are formulated as:

$$\begin{cases} P(0,t) = 84.6364\,\text{atm}, \\ T(0,t) = 40^\circ\text{C}, \end{cases} \qquad G(L,t) = \begin{cases} 102.266\,\text{mill.m}^3/\text{day}, \ t < 200\,\text{min}, \ t \geqslant 400\ \text{min}, \\ 112.266\,\text{mill.m}^3/\text{day}, \ 200\ \text{min} \leqslant t < 400\ \text{min}. \end{cases} \tag{34}$$

The remarkable thing is that the transition process starts from the 200$^{\text{th}}$ minute, and then from the 400$^{\text{th}}$ minute, which corresponds to the 40$^{\text{th}}$ and 79$^{\text{th}}$ time layer, the calculation ends after 12 hours, which corresponds to the 144$^{\text{th}}$ time layer.

We will compare the results of numerical modeling obtained using model 1 and model 2.

The Table 1 shows the maximum values of the modules of the indeterminate differences: commercial flow rate as q (mill.m^3/day), pressure as P atm and temperature as T (°C), at the 39$^{\text{th}}$, 79$^{\text{th}}$ time layers (before the transition process has been started), at the (40$^{\text{th}}$–41$^{\text{st}}$), (44$^{\text{th}}$–45$^{\text{th}}$) time layers, at the (80$^{\text{th}}$–81$^{\text{st}}$), (84$^{\text{th}}$–85$^{\text{th}}$) time layers (after the transition process has been started), at the 144$^{\text{th}}$, the last time layer.

The Figs. 1–3 show the arrangement of unknown parameters: commercial flow rate as q (mill.m^3/day), pressure as P (atm) and temperature as T (°C) in the pipeline section at the 40$^{\text{th}}$, 80$^{\text{th}}$, and 144$^{\text{th}}$ time layers calculated by means of the model 1 (the blue color) and model 2 (the yellow color).

Table 1. The maximum values of the modules of differences in terms of the flow rate, pressure and temperature (model 1 and model 2).

Time layer (number)	q	P	T
39	0.00232251	0.56747	7.54382
40	0.020842	0.611251	8.03683
41	0.0282771	0.636008	8.27864
44	0.0335407	0.686733	8.71476
45	0.0341976	0.700215	8.81933
79	0.00740013	0.850221	9.52532
80	0.0307913	0.800004	9.02821
81	0.036121	0.771965	8.78232
84	0.0390004	0.718994	8.33629
85	0.0391446	0.705665	8.22861
144	0.00096082	0.570683	7.54992

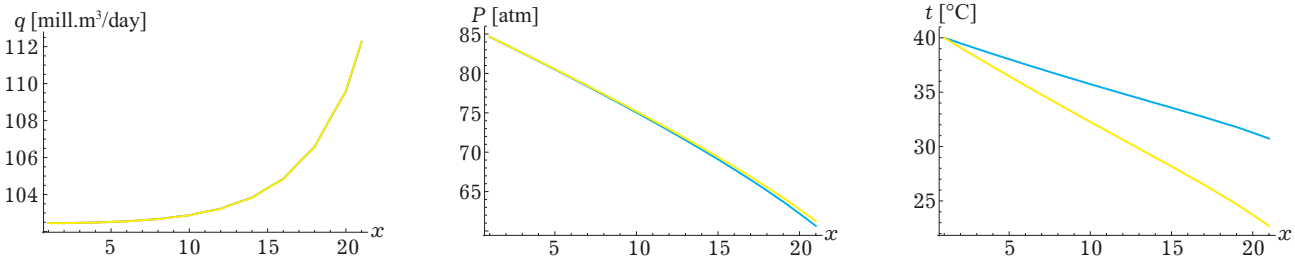

Fig. 1. Arrangement of the gas flow rate as q, pressure as P, temperature as T in the PS at the 40$^{\text{th}}$ time layer (model 1 — blue, model 2 — yellow).

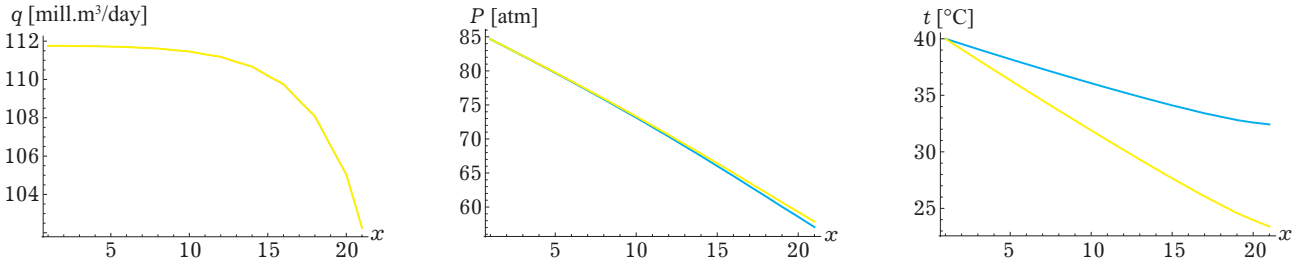

Fig. 2. Arrangement of the gas flow rate as q, pressure as P, temperature as T in the PS at the 80$^{\text{th}}$ time layer (model 1 — blue, model 2 — yellow).

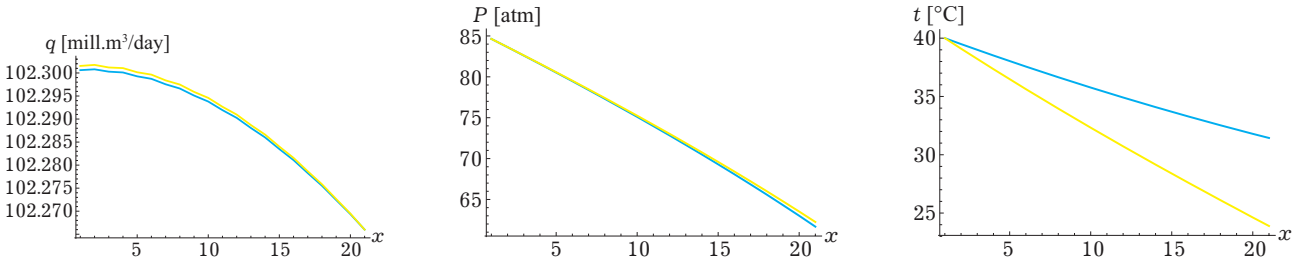

Fig. 3. Arrangement of the gas flow rate as q, pressure as P, temperature as T in the PS at the 144^{th} time layer (model 1 — blue, model 2 — yellow).

Keep in mind, that for the stationary regime defined by the NE (33), which was calculated under the model 1 and model 2, $q = 1.92015 \cdot 10^{-7}$, $P = 0.569748$, $T = 7.54274$. The Figs. 4–6 show a graph of variance of the gas flow parameters (flow rate, pressure, temperature) in terms of time where $n = 20$.

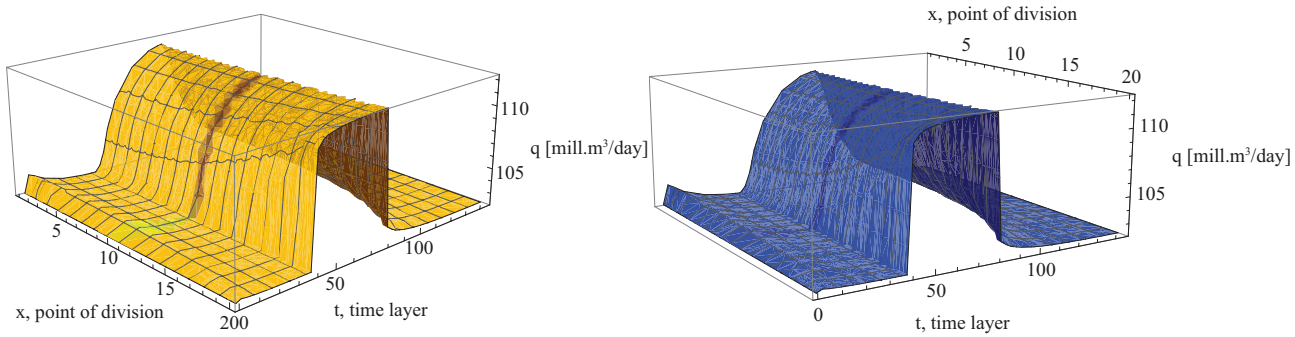

Fig. 4. Change in gas flow rate in the PS in terms of time (model 1 – yellow, model 2 — blue).

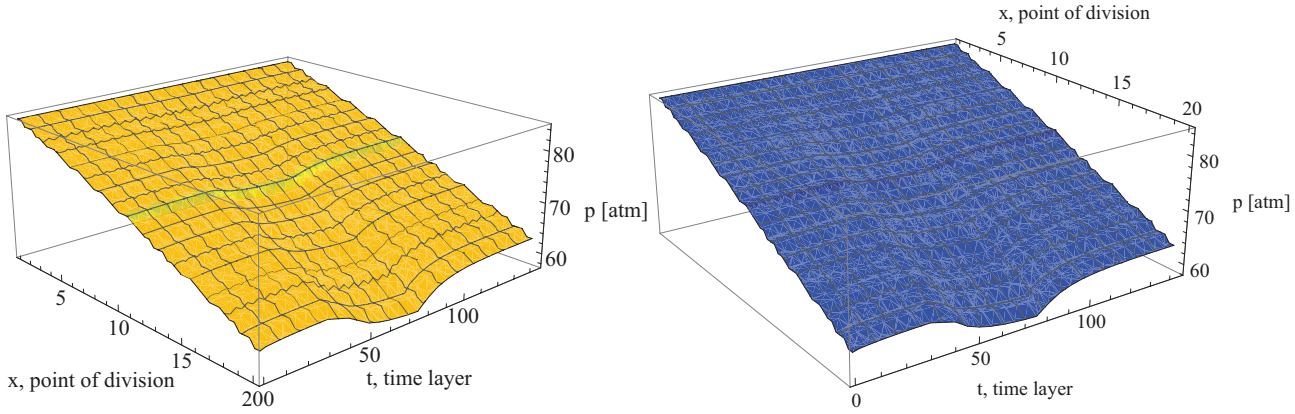

Fig. 5. Change in gas pressure in the PS in terms of time (model 1 – yellow, model 2 — blue).

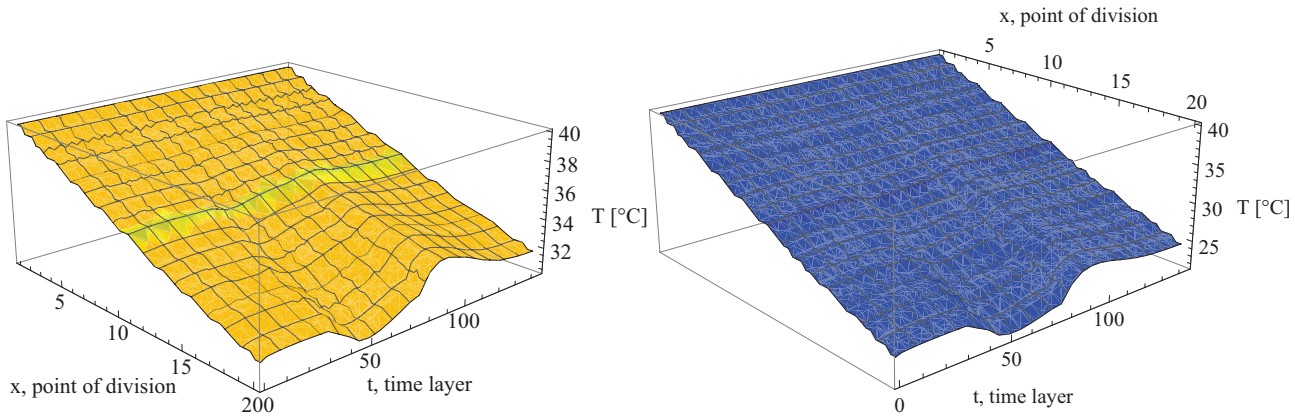

Fig. 6. Change in gas temperature in the PS in terms of time (model 1 – yellow, model 2 — blue).

As the analysis of the modeling results (Table 1, Figs. 1–3) shows, taking the Joule–Thompson effect into account affects all unknown gas parameters: flow rate, pressure and temperature. But where the flow rate differs insignificantly: in the second decimal place during the transition process and already in the fourth decimal place when the regime is almost stationary, the pressure value differs in the first decimal place both in the transition regime of gas flow (up to max. 0.850221 atm.) and at almost stationary state (0.570683 atm.). The main differences are related to temperature, where the difference reaches several degrees.

The results of numerical modeling obtained using model 1 and model 3 will be compared.

The Table 2 shows maximum values of the indeterminate difference modules: commercial flow rate as g (mill.m^3/day), pressure as P (atm) and temperature as T (°C), at the 39$^{\text{th}}$, 79$^{\text{th}}$ time layers (before the transition process has been started), at the (40$^{\text{th}}$–41$^{\text{st}}$), (44$^{\text{th}}$–45$^{\text{th}}$) time layers, at the (80$^{\text{th}}$–81$^{\text{st}}$), (84$^{\text{th}}$–85$^{\text{th}}$) time layers (after the transition process has been started), at the 144$^{\text{th}}$, the last time layer.

The Figs. 7–9 show the arrangement of unknown parameters: commercial flow rate as q (mill.m^3/day), pressure as P (atm) and temperature as T (°C) in the pipeline section at the 40$^{\text{th}}$, 80$^{\text{th}}$, and 144$^{\text{th}}$ time layers calculated by means of the model 1 (the blue color) and model 3.

Table 2. Maximum values of the difference modules in terms of the flow rate, pressure, temperature (model 1 and model 3).

Time layer (number)	q	P	T
39	0.000555952	0.00246855	0.0728544
40	0.0910354	0.0351283	3.26069
41	0.0791501	0.0478333	2.65997
44	0.0290522	0.0474618	1.37989
45	0.029533	0.042375	1.03969
79	0.0064953	0.00964285	0.272224
80	0.114385	0.297267	3.45112
81	0.102762	0.0384335	2.85515
84	0.0437087	0.0357521	1.60399
85	0.0363086	0.0312974	1.26069
144	0.00244977	0.00245885	0.0483599

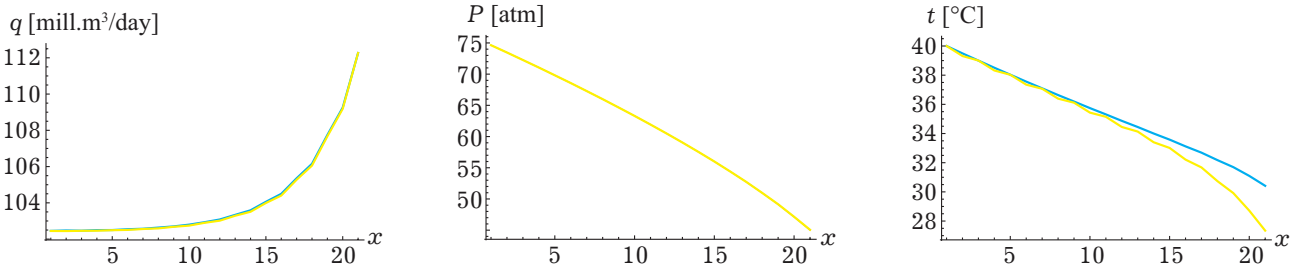

Fig. 7. Arrangement of the gas flow rate as q, pressure as P, temperature as T in the PS at the 40$^{\text{th}}$ time layer (model 1 — blue, model 3 — yellow).

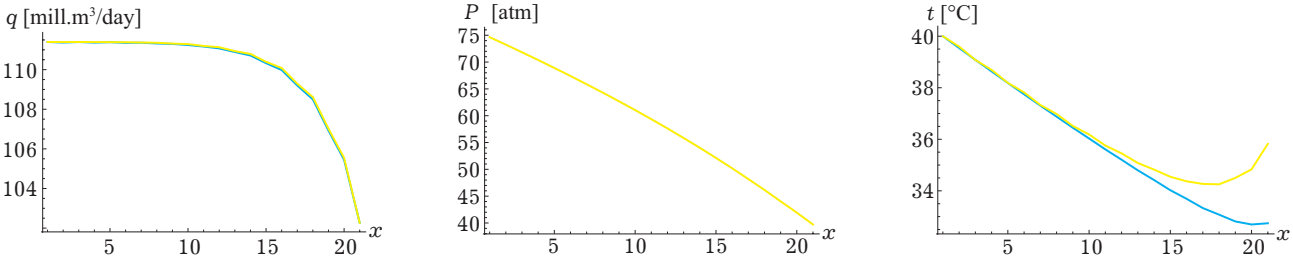

Fig. 8. Arrangement of the gas flow rate as q, pressure as P, temperature as T in the PS at the 80$^{\text{th}}$ time layer (model 1 — blue, model 3 — yellow).

Keep in mind, that for the stationary regime defined by the NE (33), which was calculated under the model 1 and model 3, $q = 2.21192 \cdot 10^{-7}$, $P = 0.784743 \cdot 10^{-4}$, $T = 0.00781894$. The Figs. 10–12 show a graph of variance of the gas flow parameters (flow rate, pressure, temperature) in terms of time where $n = 20$.

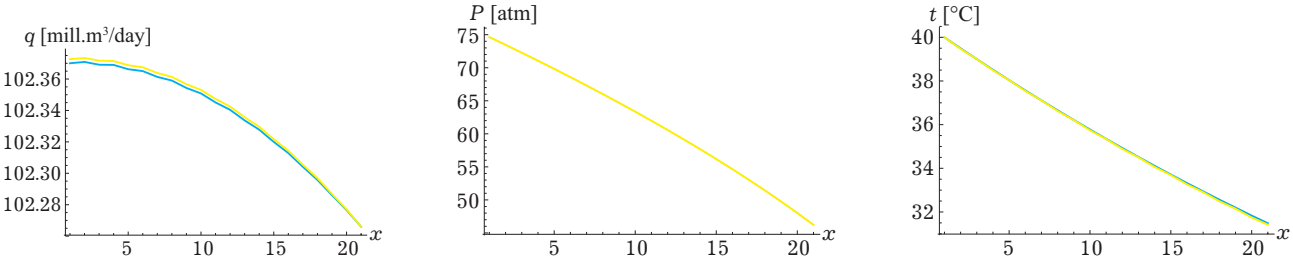

Fig. 9. Arrangement of the gas flow rate as q, pressure as P, temperature as T in the PS at the 144^{th} time layer (model 1 — blue, model 3 — yellow).

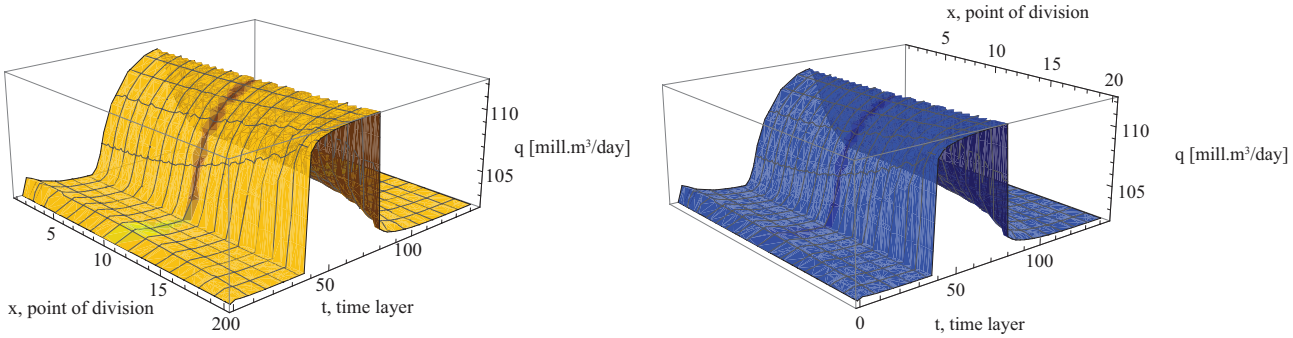

Fig. 10. Change in gas flow rate in the PS in terms of time (model 1 – yellow, model 3 — blue).

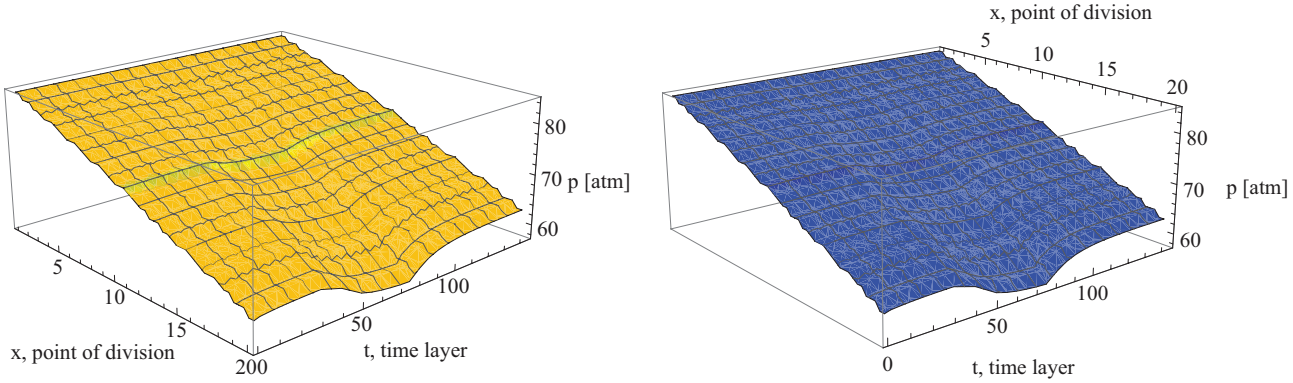

Fig. 11. Change in gas flow rate in the PS in terms of time (model 1 – yellow, model 3 — blue).

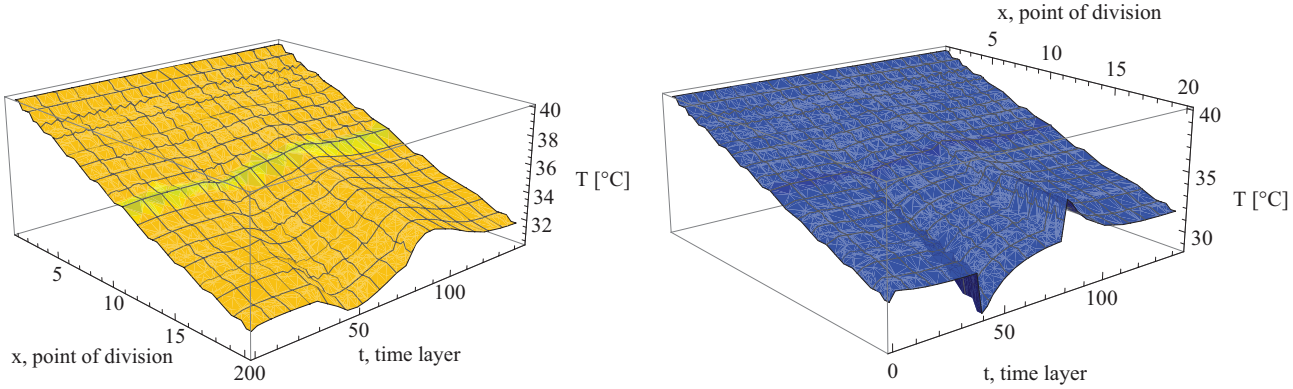

Fig. 12. Change in gas flow rate in the PS in terms of time (model 1 – yellow, model 3 – blue).

As an analysis of the modeling results (Table 2, Figs. 7–9) shows, taking into account the kinetic energy affects all unknown parameters of the gas: flow rate, pressure and temperature. But where the flow rate and pressure differ slightly: in the first or second decimal place during the transition process and in the third or fourth when the regime is almost stationary, the temperature value differs by several degrees in the transition regime of gas flow and only in the second decimal place by almost stationary state.

The situation of connecting and disconnecting a large consumer with initial conditions (33) and boundary conditions will be considered as follows:

$$\begin{cases} P(0,t) = 84.6364\,\text{atm}, \\ T(0,t) = 40^{\circ}\text{C}, \end{cases} \qquad G(L,t) = \begin{cases} 102.266\,\text{mill.m}^3/\text{day}, \ t < 200 \text{ min}, \ t \geqslant 400 \text{ min}, \\ 112.266\,\text{mill.m}^3/\text{day}, \ 200 \text{ min} \leqslant t < 400 \text{ min}. \end{cases} \tag{35}$$

which means, that the flow rate changes not for 10 (mill.m^3/day), but for 20 (mill.m^3/day).

The Table 3 shows maximum values of the indeterminate difference modules: commercial flow rate as q (mill.m^3/day), pressure as P (atm) and temperature as T (°C), at the 39$^{\text{th}}$, 79$^{\text{th}}$ time layers (before the transition process has been started), at the (40$^{\text{th}}$–41$^{\text{st}}$), (44$^{\text{th}}$–45$^{\text{th}}$) time layers, at the (80$^{\text{th}}$–81$^{\text{st}}$), (84$^{\text{th}}$–85$^{\text{th}}$) time layers (after the transition process has been started), at the 144$^{\text{th}}$, the last time layer, obtained under the model 1 and model 3.

Table 3. Maximum values of the difference modules in terms of the flow rate, pressure, temperature (model 1 and model 3).

Time layer (number)	q	P	T
39	0.000555952	0.00246855	0.0728544
40	0.165718	0.0804655	6.08443
41	0.139331	0.110728	4.92419
44	0.0506785	0.113359	2.50449
45	0.0745871	0.102485	1.87004
79	0.0120931	0.0197671	0.42173
80	0.248109	0.0487604	6.3234
81	0.23243	0.0643595	5.21266
84	0.107919	0.0599228	3.03022
85	0.0960095	0.0520082	2.42554
144	0.00488039	0.00419819	0.0957829

As the analysis of the modeling results (Tables 2–3) shows, the larger the change in the flow rate of the transported gas during the transition regime of gas flow is, the greater the difference in temperature is: when the flow rate changes for 10 (mill.m^3/day), the maximum value of difference modulus reaches 3.45112 degrees on the 80$^{\text{th}}$ time layer, and when the flow rate changes for 20 (mill.m^3/day), the maximum value of difference modulus reaches 6.3234 degrees on the same 80$^{\text{th}}$ time layer.

6. Results and discussion of the study on the effect of selecting a MM of the NNGFRs in a PS on the processes of modeling such regimes

The results of numerical modeling obtained using model 1 and model 2 (Table 1, Figs. 1–3) are compared. As the analysis of the modeling results shows, the main differences are related to temperature, and the larger the flow rate of gas transported along the PS is, the greater the difference in temperature is. The gas temperature obtained by model 2, that is, taking into account the Joule–Thompson effect, is lower than the temperature obtained by model 1. This effect is manifested along the entire length of the pipeline.

The results of numerical modeling obtained using model 1 and model 3 (Tables 2–3, Figs. 7–9) will be compared. The analysis of the modeling results shows: there are differences in the simulated unknown parameters obtained by model 1 and model 3, both in flow rate and pressure, and especially in gas temperature. This difference is maximum at the beginning of the transition process (Table 2), it decreases as the transition process has been in the stationary state (Figs. 7–8, Table 2), and it is insignificant in the case of a stationary state gas flow (Table 2, Fig. 9). In case the gas temperature is considered, then the maximum modulus of the differences between the temperature obtained by model 1 and model 3 is reached at the end of the section (Figs. 7–8). This effect, associated with a sharper change in temperature when using model 3 (taking into account the kinetic energy), manifests itself only in course of the transition process of the gas flow. The pressure drop when using model 3 results in a sharper drop in temperature (Fig. 7), the pressure increase when using model 3 results in a sharper increase in temperature (Fig. 8).

As the analysis of the modeling results (Table 2–3) shows, the larger the change in the gas flow rate in course of the transition process is, the greater the temperature difference is. This is due to the

fact that with an increase in the change in gas flow during the transition process, the pressure drop in the gas increases accordingly, which leads to a sharp change in the gas velocity and, accordingly, to a change in kinetic energy. In this case, model 3 describes the transition process more accurately.

7. Summary

The paper proposes a mathematical model of the NNGFRs in the LS, and also offers several models of NNGFRs in the PS, which are included in the general model. The model of the NNGFRs in the PS taking into account the kinetic energy is proposed for the first time. A comparative analysis of various models of the NNGFRs in the PS based on numerical modeling is also carried out.

The analysis of numerical methods for solving simultaneous equations of the MM in terms of a PS is carried out. A method based on the application of the finite difference algorithm using a uniform finite-difference implicit scheme is chosen as a numerical method.

The results of calculating the parameters of the NNGFR gas flow in the PS using various models are presented. Analysis of the results of the study on the effect of selecting a MM of the NNGFRs in a PS on the processes of modeling such regimes shows the following. The model 2 shall be selected for large diameter pipes. In this case, the Joule–Thompson effect is manifested along the entire length of the pipeline. The model 3 is more effective at modeling transients associated with large pressure drops. This will allow more accurate modeling of unknown parameters of the gas flow: flow rate, pressure, and especially temperature. Differences in temperature are observed at the beginning of the transition process and are leveled when the transition process becomes stationary.

The obtained results can be used at the stage of transfer pipeline system operation in order to develop scientifically well-founded recommendations for improving the safety and efficiency of the pipeline transportation system.

[1] Pakin A. K. Perspektivy razvitiya mirovogo rynka prirodnogo gaza. Vestnik Rossiyskogo ekonomicheskogo universiteta imeni G. V. Plekhanova. **3**, 147–153 (2016), (in Russian).

[2] Sardanashvili S. A. Raschetnyye metody i algoritmy (truboprovodnyy transport gaza). Oil and gas, Moscow (2005), (in Russian).

[3] Prytula N. Mathematical modelling of dynamic processes in gas transmission. ECONTECHMOD : An International Quarterly Journal on Economics of Technology and Modelling Processes. **4** (3), 57–63 (2015).

[4] Novyckyj N. N., Sukharev M. Gh., Tevjashev A. D. Truboprovodnyje sistemy energhetiki: Metodicheskije i prikladnyje problemy modelirovanija. Science, Novosibirsk, pp. 193–204 (2015), (in Russian).

[5] Seleznev V. E., Pryalov S. N. Metody postroeniya modelej techenij v magistral'nyh truboprovodah i kanalah: monografiya. Direct-Media, Moscow–Berlin (2014), (in Russian).

[6] Seleznev V. E., Aleshyn V. V., Pryalov S. N. Osnovy chislennogo modelirovanija magistralnyh truboprovodov. MAX Press, Moscow (2009), (in Russian).

[7] Tevyashev A. D., Husarova I. H., Churkina A. V. Effektivnyy metod i algoritm rascheta nestatsionarnykh neizotermicheskikh rezhimov transporta gaza v gazotransportnoy seti proizvol'noy struktury. Eastern-European Journal of Enterprise Technologies. **2/3** (20), 45–52 (2006).

[8] Seleznev V. E., Aleshyn V. V., Prjalov S. N. Osnovy chyseljnogho modeljuvannja maghistraljnykh ghazoprovodov. KomKnygha, Moscow (2005), (in Russian).

[9] Helgaker J. F., Müller B., Ytrehus T. Transient flow in natural gaspipelines using implicit finite difference schemes. Journal of Offshore Mechanics and Arctic Engineering. **136** (3), 031701–0317011 (2014).

[10] Ermolaeva N. N. Nestacionarnye modeli teploobmena i transportirovki gaza po morskim gazoprovodam. Transactions of the Karelian Research Centre of the Russian Academy of Sciences, Mathematical Modeling and Information Technologies Series. **8**, 3–10 (2016), (in Russian).

[11] Ermolaeva N. N. Kompyuternoe modelirovanie oledeneniya morskogo gazoprovoda i povedeniya harakteristik potoka v neustanovivshihsya rezhimah'. Bulletin of St. Petersburg University. **4** (10), 75–86 (2016), (in Russian).

[12] Husarova I. H., Melinevskyi D. V. Chislennoye modelirovaniye perekhodnykh rezhimov techeniya gaza s ispol'zovaniyem razlichnykh konechno-raznostnykh setok. Information Processing Systems. **2**, 29–33 (2017), (in Russian).

[13] Wang P., Yu B., Han D., Li J., Sun D., Xiang Y., Wang L. Adaptive implicit finite difference method for natural gas pipeline transient flow. Oil Gas Sci. Technol. **73**, 21 (2018).

[14] Zhang L. Simulation of the transient flow in a natural gas compression system using a high-order upwind scheme considering the real-gas behaviors. Journal of Natural Gas Science and Engineering. **28**, 479–490 (2016).

[15] Sung W.-P., Chen R. Application of π Equivalent Circuit in Mathematic Modeling and Simulation of Gas Pipeline. Applied Mechanics and Materials. **496**, 943–946 (2014).

[16] Husarova I. H., Korotenko A. N. Rezultaty chislennogo modelirovanija perekhodnykh rezhimov techenija gaza po uchastku truboprovoda metodom harakteristik. Information Processing Systems. **2** (153), 18–26 (2018), (in Russian).

[17] Helgaker J. F. Modeling Transient Flow in Long Distance Offshore Natural Gas Pipelines. PhD Thesis. Trondheim (2013).

[18] Zheng Y., Xiao J., Sun X., Hua H., Fang G. Application and understanding of Stoner Pipeline Simulator (SPS). Natural Gas Industry. **33**, 104–109 (2013).

[19] Zheng J. G., Chen G. Q., Song F., Ai-Mu Y., Zhao J. L. Research on simulation model and solving technology of large scale gas pipe network. Journal of System Simulation. **24** (6), 1339–1344 (2012).

[20] Husarova I. H., Boyarskaya Y. V. Klassy zadach modelirovaniya i chislennogo analiza nestatsionarnykh rezhimov raboty gazotransportnoy sistemy. Eastern-European Journal of Enterprise Technologies. **3/6** (45), 26–32 (2010), (in Russian).

[21] Galuza A., Grinberg G., Tevyasheva O., Lyubchyk L. Modeling and Optimization of Gas Transmission Systems under Uncertain Operation Conditions. 2019 9th International Conference on Advanced Computer Information Technologies (ACIT). 80–83 (2019).

[22] Pyanylo Ya., Prytula N., Prytula M., Khymko O. On an invariant of a non-stationary model of pipelines gas flow. Mathematical Modeling and Computing. **6** (1), 116–128 (2019).

Математичне моделювання нестаціонарних режимів течії газу по лінійній ділянці газотранспортної системи

Гусарова І. Г.[1], Тевяшев А. Д.[1], Тевяшева О. А.[2]

[1]*Кафедра прикладної математики,*
Харківський національний університет радіоелектроніки,
пр. Науки, 14, 61166, Харків, Україна
[2]*Кафедра комп'ютерної математики та аналізу даних,*
Національний технічний університет "Харківський політехнічний інститут",
вул. Кірпічова, 2, 61002, Харків, Україна

У статті обґрунтована актуальність моделювання нестаціонарного неізотермічного режиму течії газу по лінійній ділянці газотранспортної системи з використанням різних математичних моделей і сучасних чисельних методів. У роботі пропонується кілька моделей нестаціонарних неізотермічних режимів течії газу по ділянці трубопроводу, які входять в загальну модель, проводиться їх порівняльний аналіз на основі чисельного моделювання. Для розв'язання систем рівнянь математичної моделі по ділянці трубопроводу застосований метод скінченних різниць. Наводяться результати розрахунку параметрів газового потоку з використанням різних моделей: з урахуванням та без урахування кінетичної енергії, з урахуванням та без урахування ефекту Джоуля–Томпсона. Обговорюється питання вибору відповідної моделі. Отримані результати можуть бути використані на етапі експлуатації мереж магістральних трубопроводів з метою вироблення науково обґрунтованих рекомендацій щодо підвищення безпеки та ефективності роботи трубопровідної системи.

Ключові слова: *лінійна ділянка, нестаціонарний неізотермічний режим течії газу, моделювання, метод скінченних різниць.*